Mining Science and Technology (China) 21 (2011) 869–872

Contents lists available at SciVerse ScienceDirect

Mining Science and Technology (China)

journal homepage: www.elsevier.com/locate/mstc

Land subsidence monitoring by D-InSAR technique

Fan Hongdong *, Deng Kazhong, Ju Chengyu, Zhu Chuanguang, Xue Jiqun

China University of Mining & Technology, Key Laboratory for Land Environment and Disaster Monitoring of SBSM, Xuzhou 221116, China

ARTICLE INFO

Article history:
Received 18 March 2011
Received in revised form 20 April 2011
Accepted 13 May 2011
Available online 23 December 2011

Keywords:
InSAR
"Two-pass" differential
Land subsidence
Confined water level
Groundwater

ABSTRACT

Nowadays, the researches of using Differential Interferometric Synthetic Aperture Radar (D-InSAR) technique to monitor the land subsidence are mainly on how to qualitatively analyze the subsidence areas and values, but the analysis of subsidence process and mechanism are insufficient. In order to resolve these problems, 6 scenes of ERS1/2 images captured during 1995 and 2000 in a certain place of Jiangsu province were selected to obtain the subsidence and velocities in three time segments by "two-pass" D-InSAR method. Then the relationships among distributions of pumping wells, exploitation quantity of groundwater, and confined water levels were studied and the subsidence mechanism was systematically analyzed. The results show that using D-InSAR technique to monitor the deformation of large area can obtain high accuracies, the disadvantages of classical observation methods can be remedied and there is a linear relationship among the velocities of land subsidence, the water level and the exploitation quantity.

1. Introduction

As a new method for obtaining regional subsidence, compared with the conventional monitoring methods, D-InSAR technique has some advantages in some research fields, such as earthquake deformation, land subsidence, volcanic activity, landslide of mountains and so on [1–16]. Therefore, using D-InSAR technique to monitor the land deformation has become a research focus at home and abroad nowadays. Since Gabriel and his colleagues firstly proved that D-InSAR technique could detect the land deformation of centimeter level, a lot of researches on land subsidence have been developed by many scientists of different countries and some achievements were obtained [3]. Using ERS1/2 Tandem and JERS-1 L band images captured between 1993 and 1995, combined with GIS, some quantitative analysis was made on land subsidence in Appin area caused by long wall coal mining [4]. Hoffmann studied the land subsidence of Antelope valley in California caused by pumping the geothermal water to generate power [5]. Bernhard used the interferometric point targets analysis technique to obtain the land subsidence of Lost Hills oil area in California [6]. Using D-InSAR technique, Gong studied the land subsidence caused by groundwater over-exploitation of Cangzhou in Hebei province [7].

However, the present researches of using D-InSAR to monitor the subsidence are mainly in how to analyze the subsidence areas and values qualitatively, but the analysis of process and mechanism of the subsidence are obviously insufficient. In addition, the area studied in this paper, the recorded maximum level of subsidence had been over 881 mm during the past 30 years, and some serous damages are continuing. Although the leveling observation with a high precise was used to monitor the subsidence all the time, lots of control points were damaged every year, and a lot of manpower and material resource have been consumed for the observation and supplementation of control points. Therefore, in order to remedy the disadvantages of D-InSAR and classical observation methods, the subsidence and velocities in three time segments were obtained by "two-pass" D-InSAR method, and then according to the distribution of pumping wells, the exploitation quantity of the groundwater, the confined water level and the regression equations were established and the subsidence mechanism was systematically analyzed.

2. D-InSAR technique

D-InSAR technique is a method where phase information of radar carrier is used to obtain the land deformation. In the repeat pass mode, if the land deformation happened during the capture of the two images, the interferometric fringes generated by these two images mainly include some phase information as follows [17]:

$$\phi = \phi_{topo} + \phi_{disp} + \phi_{atmo} + \phi_{flat} + \phi_{noise} \quad (1)$$

where ϕ_{topo} is the topographic phase; ϕ_{disp} is the phase change due to movement of the pixel in the satellite line-of-sight direction; ϕ_{atmo} is the phase equivalent of the difference in atmospheric retardation between passes; ϕ_{flat} is the phase caused by reference plane;

* Corresponding author. Tel.: +86 15862165361.
E-mail address: cumtfanhd@163.com (H. Fan).

1674-5264/$ - see front matter © 2011 Published by Elsevier B.V. on behalf of China University of Mining & Technology.
doi:10.1016/j.mstc.2011.05.030

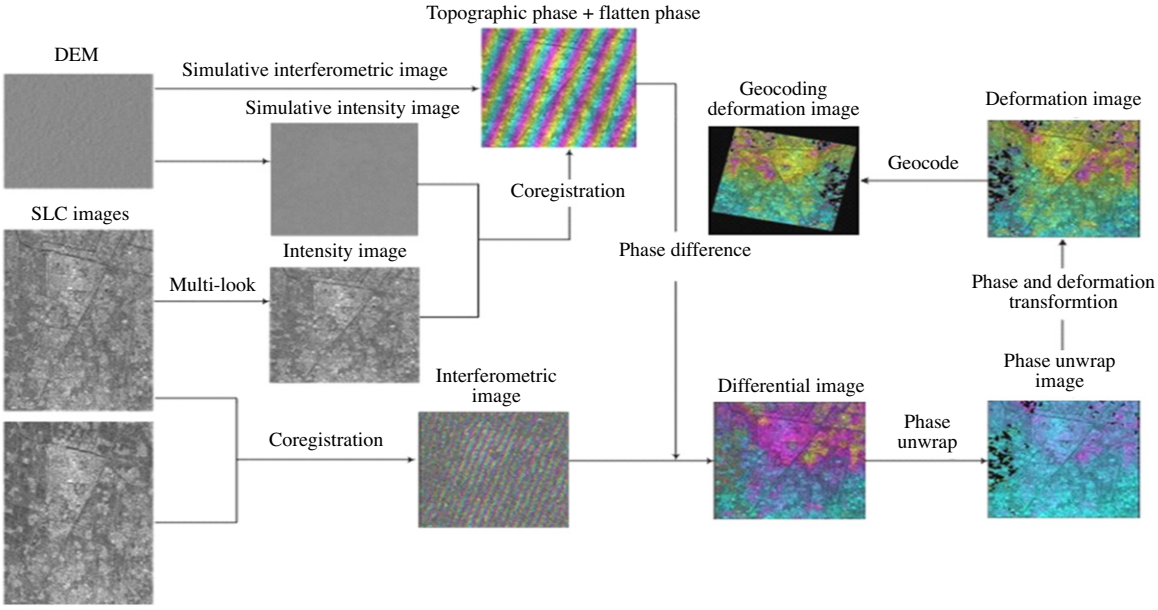

Fig. 1. Process steps of "two-pass" differential method [19].

ϕ_{noise} is the noise term due to variability in scattering from the pixel, thermal noise and coregistration errors.

How to get ϕ_{disp} is the problem to be resolved by D-InSAR technique, and ϕ_{topo} is the main factor to be removed. The "two-pass" D-InSAR and SRTM DEM, whose precision is better than 1:25,000 topographic map [18] were used in this paper. The process steps are shown in Fig. 1.

Table 1
Interferometric SAR images used for experiment.

Serial number	Master image	Slave image	$B_{\parallel}$ (m)	$B_{\perp}$ (m)	Time interval (d)
1	19,950,701	19,960,825	66	154	421
2	19,970,706	19,980,826	10	70	385
3	19,981,004	20,000,521	1	−64	595

3. Results and discussion

The experimental area is located in the North of Jiangsu province, and the water supply source is mainly from upper aquifer of the quaternary system. Due to being exploited nearly 30 years, the level of groundwater decreased continuously, and the land subsidence is quite serious. The observation data have been accumulated for 20 years since the observation points of land subsidence were established in 1988 [20]. Until 2007, the recorded maximum level of subsidence in this area had been over 881 mm. Now, the subsidence is continuing and has caused damages to some buildings and underground pipelines in local area. With the continuous extension of land subsidence, the buildings, underground pipelines, storm drainage and flood control in a larger range will be seriously threatened, and environmental geological hazards will be induced. Due to the traditional monitoring methods having some disadvantages such as high cost, long period, and insufficient discrete points and so on, these methods are difficult to meet the requirements for real time and monitoring large area by plane. Therefore, a new method called D-InSAR technique was tried to obtain the land deformation. Six scenes of ERS1/2 images (Table 1) captured between 1995 and 2000 were selected to obtain the subsidence and velocities in three time segments, and the results were compared with the measured data.

The overlapping charts of the differential phase and intensity images of the three time segments are shown in Fig. 2. Due to long time baselines, the interferometric images are not very good, but the coherences of research place are mostly bigger than 0.3, so the phase unwrapping results are reliable. Due to the perpendicular baseline of Fig. 2a longer than the other two images, its coherence is worse. Because of the limited space, only the comparison between the results calculated by D-InSAR and ground measurements during October 1998 to May 2000 are shown in Fig. 3, and they are nearly the same in deformation trend and values. Therefore, it is proved that using D-InSAR to monitor the land deformation is effective and reliable. One thing should be introduced necessarily. Due to ERS image with a lower resolution about 4 m × 20 m, so if you want to make the monitoring points on D-InSAR image and the observation points nearly have a one-to-one correspondence, two methods such as oversampling technique or interpolation method after the geocoding step can be employed. The former method is to use the oversampling technique to improve the resolution of range direction before the interferogram is generated, after that, the resolution of 4 m × 4 m can be obtained, and then the subsequent process can be operated. The latter method is to use the relationship between the neighbor pixel coordinates after geocoding step to interpolate the corresponding deformation values of D-InSAR. The latter method was chosen in this paper.

The contour maps of surface subsidence calculated by D-InSAR technique in the three time segments are shown in Fig. 4, and they are overlapped with the pumping wells. In this experiment, only the phases with coherences bigger than 0.3 were unwrapped, and then some small isolated islands outside the urban were removed. From Fig. 4, some conclusions can be obtained as follows: during July 1995 to August 1996, the area with good coherences were relatively smaller, the whole region was subsidized, and the subsidence values of the urban centre with more pumping wells were between −10 and −20 mm, and the maximum was lower than −20 mm; during July 1997 to July 1998, the position of the

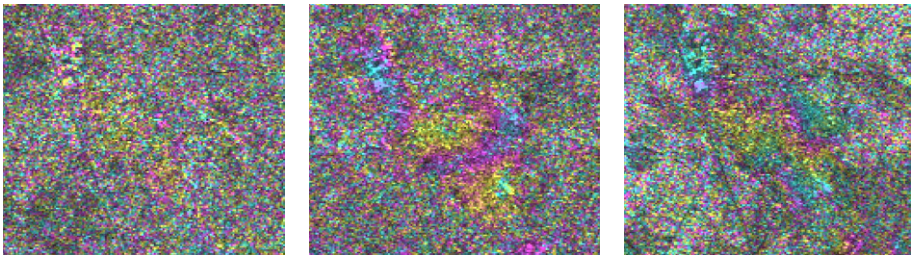

(a) 199507-199608 (b) 199707-199807 (c) 199810-200005

Fig. 2. Overlapping charts of differential phase and intensity images.

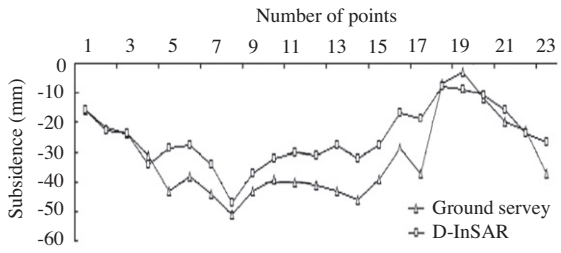

Fig. 3. Comparison between D-InSAR and ground measurements (199,810–200,005).

pumping wells could be covered by the area with good coherences, the subsidence values of the urban centre were between −10 and −30 mm, and 1–2 pumping wells near the subsidence areas were lower than −30 mm, so it could be seen that the pumpages of these wells were relatively bigger; during October 1998 to May 2000. The north of the urban presented surface uplift with lower than 10 mm, while the subsidence values in the south of the urban were lower than −30 mm. On the one hand this case might be caused by phase unwrapping or atmospheric errors, on the other hand, if the positions of pumping of the wells and time segment (with long time interval and from dry season to wet season) are considered, then, this subsidence and uplift case of this area was likely presented.

4. Analysis of subsidence mechanism

Based on the Terzaghi's principle of effective stress, an equation can be established as follows:

$$\sigma = \sigma_1 + \mu \tag{2}$$

where σ is the total vertical stress of stratum at a depth of h; μ is the stress of interstice water; σ_1 is the baring stress of soil skeleton, namely the effective stress.

The reason that the compression distortion of stratum is formed can be concluded as follows: before groundwater exploitation, the overlying load of aquifer was undertaken by the aquifer skeleton and groundwater, but after groundwater exploitation, due to the descended levels of groundwater, the μ decreased, but σ was invariable, so σ_1 of the aquifer would increase consequentially. Therefore, the skeleton was compressed because of the additive effective stress on it. When the compression of soil granule was ignored, the compression of the skeleton was actually the compression of stratum interstice, and that induced the subsidence of the ground. In theory, when the groundwater is exploited, the ground subsidence will appear at the same time, but the consolidation deformation will not be generated in aquifer and for a short time groundwater level will descend, this can be considered as recoverable deformation. Therefore, when the exploitation was finished, the groundwater level returned to the original state, the ground

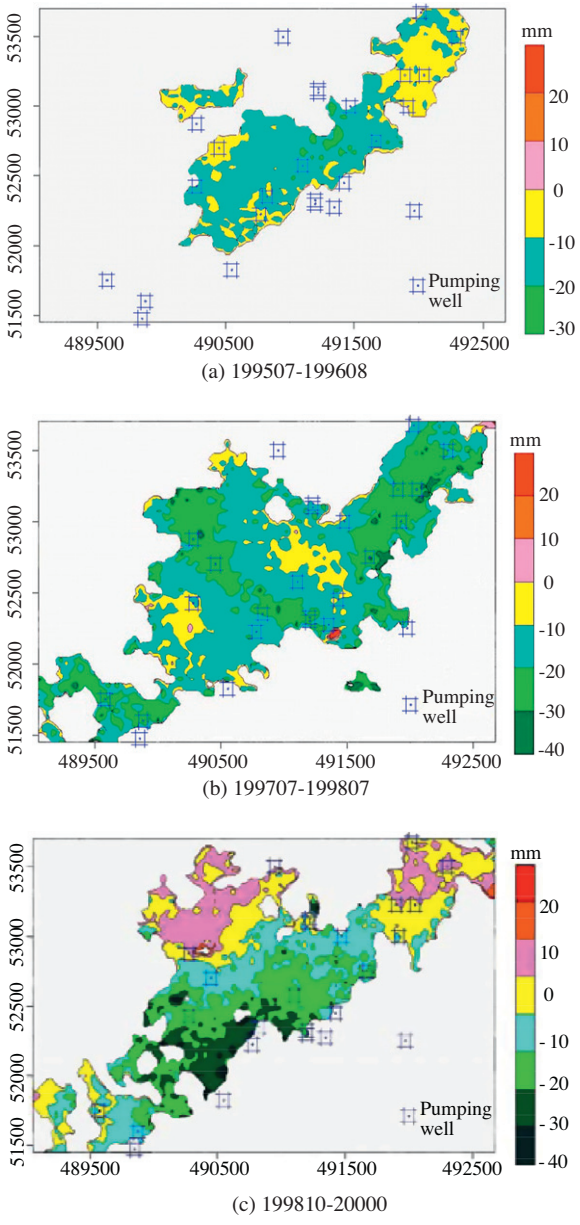

Fig. 4. Contour maps of surface subsidence overlapped with the pumping wells.

Table 2
Parameter list correlated with land subsidence.

Time segment	Average of confined water level (m)	Subsidence obtained by D-InSAR (mm)	Subsidence velocity (mm/10 days)	Average quantity of groundwater exploited (10^5 m^3/month)
9507–9608	29.73	−21.0	−0.4988	0.37412
9607–9807	28.13	−23.0	−0.5974	0.39499
9810–0005	27.21	−47.0	−0.7899	0.41833

subsidence nearly not appeared and there was just the instantaneous distortion; but if the groundwater level keeps descending for a long time, the ground subsidence will appear because of the continuous deformation in aquifer.

Based on the former analysis, there is a corresponding relationship between ground subsidence and confined water level in the time domain; similarly, there is corresponding relationship between the height of the confined water level and the exploited groundwater quantity (some factors such as rainfall, runoff replenishment and so on are ignored). Due to insufficient observed data, the average of confined water level and exploited quantity were collected only in Qicun point (Table 2), together with the ground subsidence quantity obtained by D-InSAR, the regressive analysis was processed.

Based on the data shown in Table 2, the linear regression relationship can be established between h and Q:

$$h = -56.664Q + 50.785 \quad (R^2 = 0.9655) \tag{3}$$

The regression relationship between v and h can be shown as follows:

$$v = 0.1095h - 3.734 \quad (R^2 = 0.8896) \tag{4}$$

The correlation coefficients between confined water level and average exploitation and ground subsidence velocities are 0.9655, 0.8896, respectively, so the regression equations are relatively reliable. Based on Eqs. (3) and (4), two conclusions can be obtained as follows: (1) There is a linear relationship among the velocities of land subsidence, the water level and the exploitation quantity. (2) With the reduction of exploitation quantity, the water level rises, and the velocities of land subsidence decrease; with the increase of exploitation quantity, the water level drops, and the velocities of land subsidence increase.

5. Conclusions

(1) Six scenes of ERS1/2 images captured between 1995 and 2000 in a certain place of Jiangsu province were processed, and the subsidence in three time segments were obtained, compared with the ground observation data, the results are nearly the same in subsidence trend and quantity, so this proves that using D-InSAR technology to monitor the ground subsidence is more effective.

(2) The subsidence velocities in the three time segments were calculated using the subsidence quantity obtained by D-InSAR, considering the distribution of pumping wells, the exploitation quantity of groundwater, and the confined water level, the regression equations were established, and then the ground subsidence mechanism was systematically analyzed. A conclusion can be obtained as follows: there is a linear relationship among the velocities of land subsidence, the water level and the exploitation quantity, and with the reduction of exploitation quantity, the water level rises, and the velocities of land subsidence decrease; with the increase of exploitation quantity, the water level drops, and the velocities of land subsidence increase.

Acknowledgments

Thanks to Professor Feng Qiyan and Ph.D. Meng Lei of the China University of Mining and Technology for providing us with the ground observation data. Financial support for this work, provided by the National Natural Science Foundation of China (No. 41071273), the Fundamental Research Funds for the Central Universities (No. 2010QNA21) and the Project Sponsored by the Scientific Research Foundation of Key Laboratory for Land Environment and Disaster Monitoring of SBSM (No. LEDM2011B07), are gratefully acknowledged.

References

[1] Wang R, Xia Y, Grosser H, Wetzei HU, Kaufmann H, Zschau J. The 2003 BAM (SE Iran) earthquake: precise source parameters from satellite radar interferometry. J Geophys Res 2004;159(3):917–22.
[2] Chang ZQ, Gong HL, Zhang JF, Gong LX. A feasible approach for improving accuracy of ground deformation measured by D-InSAR. J Univ Min Technol 2007;17(2):262–6.
[3] Gabriel AK, Goldstein RM. Crossed orbit interferometry: theory and experimental results from SIR-B. Int J Remote Sens 1988;9(5):857–72.
[4] Ge LL, Chris R, Han SW, Zebker H. Mining subsidence monitoring using the combined InSAR and GPS approach. In: The 10th FIG international symposium on deformation measurements, Orange: CD-ROM; 2001. p. 1–10.
[5] Hoffmann J. The application of satellite radar interferometry to study of land subsidence over developed aquifer systems. PhD dissertation, California: Stanford University; 2003.
[6] Rabus B, Werner C, Wegmueller U, Mccardle A. Interferometric point target analysis of RADARSAT-1 data for deformation monitoring at the Belridge/Lost Hills oil fields. In: 2004 Geoscience and remote sensing symposium. Anchorage: Country of Publication; 2004. p. 2611–3.
[7] Gong LX, Zhang JF, Guo QS. Measure groundwater pumping induced subsidence with D-InSAR. In: 2005 Geoscience and remote sensing symposium. Seoul: Country of Publication; 2005. p. 2169–71.
[8] Lu Z, Freymueller J, Meyer D, Mann D. Synthetic aperture radar interferometry of Okmok volcano, Alaska: Radar observations. J Geophys Res 2000;105(10):10791–806.
[9] Chen GH, Shan XJ, Wooil M, Kyung RK. A modeling of the magma chamber beneath the Changbai Mountains volcanic area constrained by InSAR and GPS derived deformation. J Geophys 2008;51(4):1085–92.
[10] Fruneau B, Achache J, Delacourt C. Observation and modeling of the Saint-Étienne-de-Tinée landslide using SAR interferometry. Tectonophysics 1996;265(3):181–90.
[11] Fan QS, Tang CL, Chen Y, Zhang XD. Applications of GPS and InSAR in monitoring of landslide studies. Sci Surv Map 2006;31(5):60–2.
[12] Zhou HF, Zhang JF, Hu LY, Luo Y. Co-seismic deformation field and parameters inversion of the Yushu earthquake from InSAR. J Geo-Information Sci 2011;13(3):418–23.
[13] Yao X, Zhang YS, Yang N, Xiong TY. D-InSAR observation of earth surface deformation in the MS_7.1 Yushu earthquake. J Geomech 2010;16(2):129–36.
[14] Ng AH, Ge LL, Yan YQ, Li XJ, Chang HC, Zhang K, et al. Mapping accumulated mine subsidence using small stack of SAR differential interferograms in the Southern coalfield of New South Wales, Australia? Eng Geol 2010;115:1–15.
[15] Yang CS, Zhang Q, Zhao CY, Ji LY, Zhu W. Monitoring mine collapse by D-InSAR. Min Sci Technol 2010;20(5):696–700 [in Chinese].
[16] Zhao CY, Zhang Q, Yang CS, Zou WB. Integration of MODIS data and Short Baseline Subset (SBAS) technique for land subsidence monitoring in Datong, China. J Geodyn 2010;11:1–8.
[17] Fan HD, Deng KZ, Xue JQ, Zhu CG. An experimental research on using time series SAR images to monitor mining subsidence. Saf Coal Mines 2011;42(2):15–9 [in Chinese].
[18] Dong YS, Ge LL, Chang HC, Zhang Z. Mine subsidence monitoring by differential InSAR. Geomatics Inf Sci Wuhan Univ 2007;32(10):888–91.
[19] Fan HD, Study on several key algorithms of InSAR technique and its application. PhD dissertation, Xuzhou: China University of Mining and Technology; 2010.
[20] Feng QY, Liu GJ, Meng L, Fu EJ, Zhang HR, Zhang KF. Land subsidence induced by groundwater extraction and building damage level assessment – a case study of Datun, China. J Univ Min Technol 2008;18(4):556–60.